Water saturation of coal samples during long-term impregnation

Water saturation of coal samples during long-term impregnation

Volodymyr Yelisieiev[1], Vasyl Lutsenko[1,3], Tetiana Tepla[1], Tetiana Ruzova[2] and Michael Harasek[2]

[1]Institute of Geotechnical Mechanics named by N. Poljakov of National Academy of Sciences of Ukraine, Simferopolska Str., 2a, Dnipro, 49005, Ukraine
[2]TU Wien, Institute of Chemical, Environmental and Bioscience Engineering, Karlsplatz 13, Vienna, 1040, Austria

[3]Corresponding author: VILutsenko@nas.gov.ua

Abstract. The paper investigates applicability of two mathematical models developed by the authors for calculating the process of long-term impregnation of coal samples. A distinctive feature of the studied samples is low porosity. Considered models are based on single- and three-channel representation of the internal structure of a porous medium. These models were previously used to study the process of long-term impregnation of highly porous materials. At the same time, the three-channel model in most cases showed much better agreement with experimental data. This study revealed some features of these models associated with approximation of the experimental data obtained for the low porous samples. These features consist in the presence of rather small (in some cases) errors in the processing of experimental points by means of single-channel model. At the same time, the refinements obtained by means of multi-channel model cause only slight error decrease. The results suggest that the channel distributions along the radial direction of the investigated coal samples are narrow and have a pronounced peaks close to the obtained average values.

1. Introduction

The processes of impregnation and dehydration of various porous media have been studied for a long time [1–3], however, recently, interest in these issues gained new impetus due to some special features of long-term impregnation process and its duration. It is established that the total dimensionless impregnation time is about 10^5–10^6 [4, 5] that may significantly exceed the generally accepted value. Our experiments with different materials [6] also confirm these data.

In this paper we present calculation of the water saturation process for the coal samples; our findings are based on the experimental data and theoretical provisions [7]. The porous structure of the coal significantly differs from the samples studied in [6, 7]. This difference lies both in the pore system geometrical (isotropic vs. non-isotropic, fractured vs. channel) and physicochemical (wettable vs. non-wettable surface, soluble vs. swelling washed internal areas) features of the pore walls. Besides, there were attempts to influence the internal structure of the channels in the test samples: coal samples were impregnated with 3% hydrogen peroxide. Hydrogen peroxide is a substance with relatively high chemical activity which used for furnace coal desulfurization [8]. Authors performed impregnation of coal samples with water before and after their treatment with hydrogen peroxide. Generally, subject to careful methodological work, this approach can provide interesting material for evaluating the change in the pore

space in the structure of the investigated samples. However, in this study special attention was given to mathematical evaluation of the correspondence between the theoretical and experimental curves.

Thus, the aim of this study is to present new experimental results for the process of long-term impregnation of coal lumps and to perform mathematical evaluation of these results using single- and three-channel models of the pores space.

2. Methods

Experimental procedure was very similar to that presented in [6]. As methodology is completely described there, we will not provide it in this paper. Eighteen (18) free-form samples from 0.015 to 0.095 kg were taken for experiment. Some of them were fragmented during the experiment and excluded. Eight (8) samples were treated with 3% hydrogen peroxide.

One of the biggest challenges of filtration flows and, in particular, impregnation processes, is to establish relationship between flow parameters and pore system geometry of the investigated material. As a rule, a theory is based on some ideas about the structure of the pore space. These ideas are well-studied and covered in the literature, for example [9 – 11]. Moreover, there were several attempts of computer simulation of the pore space [12].

In this article, the analysis of the impregnation process is carried out on the basis of a mathematical model of the bubble displacement in capillary channel. This model is applied for simulation of impregnation process [7] with single-channel and three-channel representations of a porous medium. The three-channel representation allows to improve the approximation of impregnation process for various highly porous materials investigated in this study [7].

Similarly to [7], the calculation procedure consisted of two stages. At the first stage, average channel radius R_{Sr} is assigned to certain values. Then, by numerically solving the corresponding differential equations, the capillary rise curves are calculated and the squared error $\Delta_{\mathrm{I}} = \sum_{K=1}^{N}\left(w_K^{\mathrm{E}} - w_K^{\mathrm{R}}\right)^2$ is estimated. Squared error between corresponding actual w_K^{R} and estimated w_K^{E} water saturation values is evaluated in entire time interval (at timepoints were measurements were taken). After the minimum error Δ_{I} has been evaluated, meaningful value R_{Sr} is specified. So, at the first stage a single-channel mathematical model describing experimental saturation curve is established.

At the second stage, we performed calculations according to three-channel model, in which the whole pore system is represented as a set of three unconnected channels of different radii. In this case, the following relations should be satisfied

$$R_{\mathrm{Sr}} = \alpha R_{\mathrm{Min}} + \beta R_{\mathrm{Sr}} + \gamma R_{\mathrm{Max}}, \quad (1)$$

$$\alpha + \beta + \gamma = 1, \quad (2)$$

where R_{Min}, R_{Sr}, R_{Max}, and m are respectively the minimum, average and maximum channels radius; α, β, γ – dimensionless coefficients that determine the contribution of the corresponding channels in the whole system.

Further we estimate one of the unknown variables in equations (1), (2) for specified maximum and minimum radii. Actually, the issue was to choose such γ value so that the squared error Δ_{III} for three channels also reached the minimum. As a result, the theoretical consideration is reduced to finding the closest approximation of the experimental curve not by a formal set of functions, but by a certain class of curves specified from the mathematical model of the impregnation process. This approach allows to obtain at least an approximate distribution of pore channels and to assess the validity of the mathematical model and the possibility of its refinement.

3. Results and discussion

Figures 1-8 show experimental data and curves that approximate them. Approximating curves are obtained according to [7].

For convenience, each figure is presented in two parts. In the first part (a) all experimental data are given, and the second part (b) shows only initial period (about one tenth of the total time of experiment).

The designations of the experimental points and the curves approximating them in all figures are the same and have the following form. P-curves describe process of impregnation with hydrogen peroxide, A-curves A represent process of water impregnation before hydrogen peroxide treatment. B-curves correspond to water impregnation after hydrogen peroxide treatment. Curves marked with index 1 correspond to single-channel model approximation, curves marked with index 2 – to three-channel model approximations. Experimental points are the following: ▲ – impregnation with hydrogen peroxide, ■ – impregnation with water before using hydrogen peroxide, ♦ – impregnation with water after using hydrogen peroxide. Different figures may present a different set of experimental points and curves approximating them.

Further in the text information common to all figures is omitted.

As follows from the experiments, water saturation of the studied samples is rather low. Basically, it does not reach 0.1. The exceptions are the third and fifth samples, where w slightly exceeds the specified value, but for the first and eighth samples w is much less. These findings show the physical differences in the pore systems of the investigated coal specimens. In our opinion, behavior of water saturation value after hydrogen peroxide treatment is very important. As it follows from the 1, 3-8 only for the first sample (figure 1) points, corresponding to water saturation values, are lower than the previous ones obtained using hydrogen peroxide.

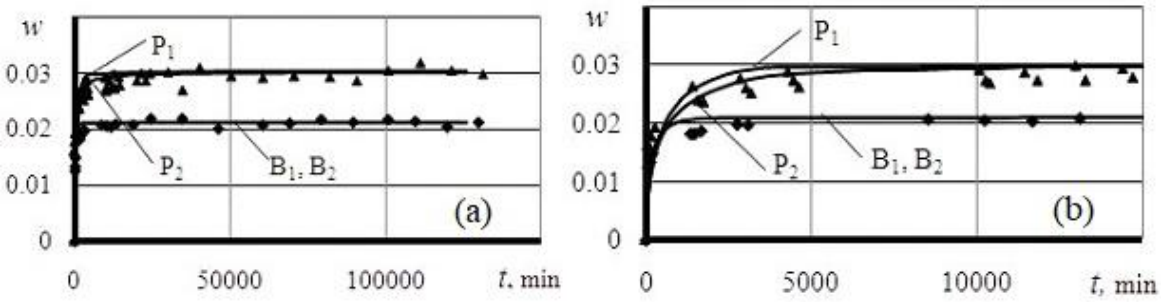

Figure 1. Impregnation curves for the 1st sample.

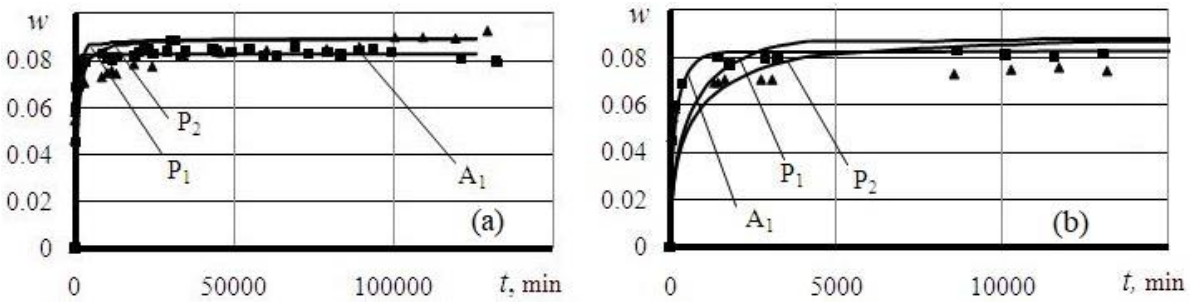

Figure 2. Impregnation curves for the 2nd sample.

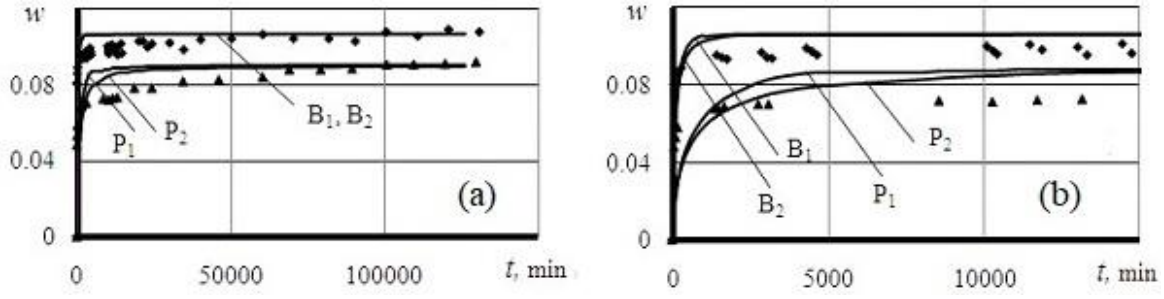

Figure 3. Impregnation curves for the 3rd sample.

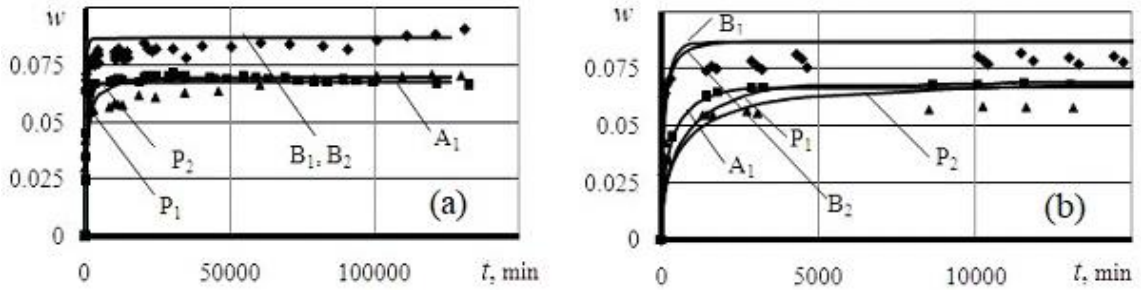

Figure 4. Impregnation curves for the 4th sample.

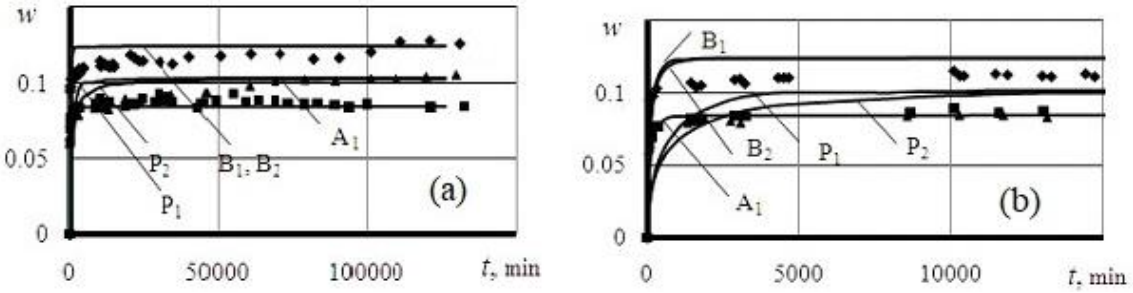

Figure 5. Impregnation curves for the 5th sample.

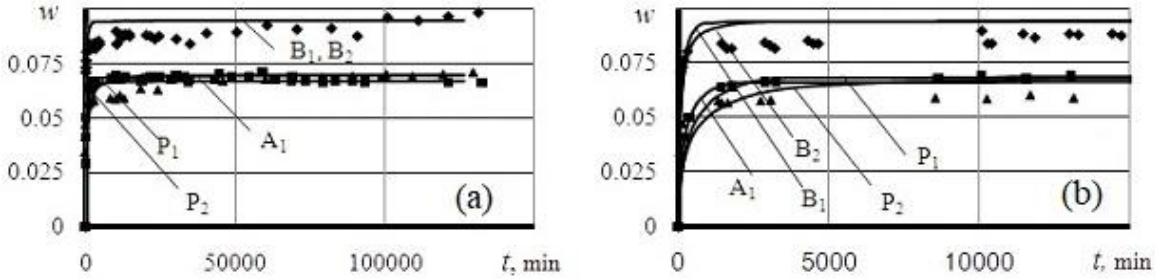

Figure 6. Impregnation curves for the 6th sample.

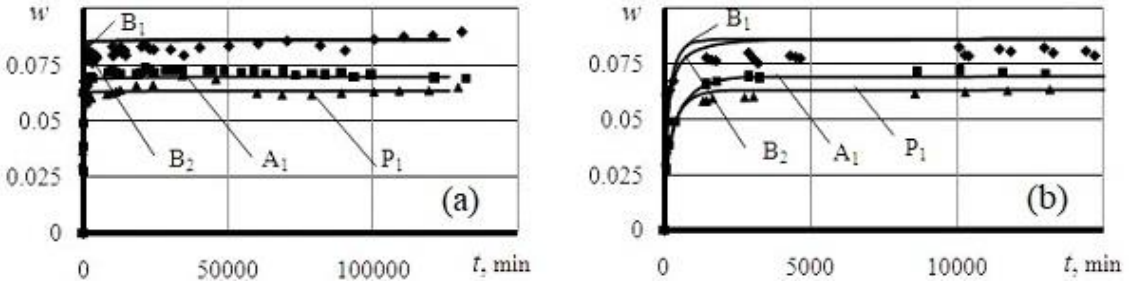

Figure 7. Impregnation curves for the 7th sample.

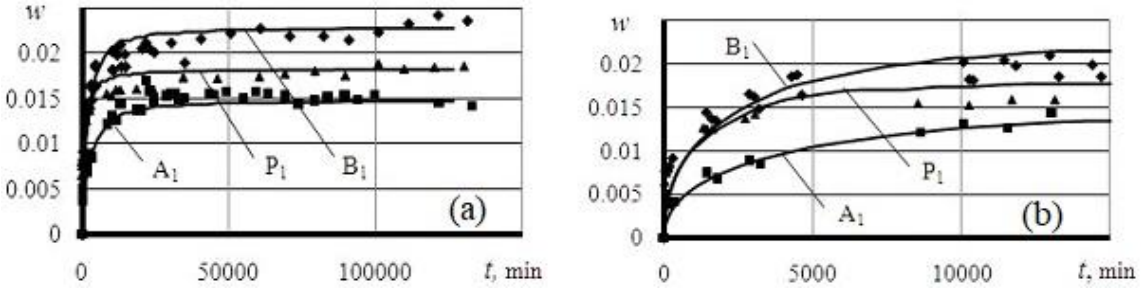

Figure 8. Impregnation curves for the 8th sample.

In all other cases (figures 3-8) they (rhombus) is above the triangles (i.e. B-curves are above P-curves). The increase in water saturation may be naturally explained by the fact that some substances located between coal crystals, in particular sulfides react with H_2O_2 and with acid fraction, then they enter the solution, diffusing through the channels. It leads to erosion of the pore walls and, probably, causes the opening of some small blind or dead-end pores to the surface.

This process to some extent corresponds to the process of dissolution of the pore channels walls. However, according to Lykov [1], the process of such dissolution may be preceded by a swelling. According to [13], swelling effect is induced by penetration of the solvent into coal structure. It is associated with the penetration of the active substance, in particular water and peroxide, into the organic layers and increase of their volumes. If no extraction (nothing is transferred into solvent) and no diffusion take place, this plug is stable and may block the pore channels for a long time, although the swelling process itself is generally reversible. Thus, both processes are associated with the structure of the pore space and the substances inside the coal. And this, in turn, depends on the coal deposit's nature and time of its metamorphism.

Correlation between hydrogen peroxide saturation and water pre-impregnation curves is also of great interest. In figure 7, the experimental water saturation points (points ■ and A- curves) are slightly higher than points corresponding to peroxide impregnation (points ▲ and P-curves). Probably, this is caused by swelling processes in the first stage of the experiment. In other experiments (figures 2, 4 - 6, 8) peroxide saturation curves are higher than the first curves, this fact suggests greater activity of dissolution process and a more pronounced effect of hydrogen peroxide.

The results of mathematical processing in the figures are described by curves A, P and B. They are obtained according to the calculation procedure mentioned in section 2 and described in [7]. At the same time, it is assumed that all pore channels are completely filled with solution, i.e. relative water saturation value for these channels at the end of the process is taken equal to one or about one. In practice, we averaged the last five water saturation values for each sample and then divide all the experimental data by corresponding average value. After that, average pore radius is specified and calculations according to three-channel model of the porous space (second stage) are performed. As a result of calculations, the following values are obtained.

First sample (figure 1). Curve P_1: $R_{Sr} = 10 \cdot 10^{-7}$ m, $\Delta_I = 0.0655$. Curve P_2: $R_{Min} = 8 \cdot 10^{-7}$ m, $R_{Max} = 12 \cdot 10^{-7}$ m, $\Delta_{III} = 0.0378$ (α =0.308, β = 0.352, γ = 0.34). Curve B_1: $R_{Sr} = 5.4 \cdot 10^{-7}$ m, $\Delta_I = 0.195$. Curve B_2: $R_{Min} = 3 \cdot 10^{-7}$ m, $R_{Max} = 11 \cdot 10^{-7}$ m, $\Delta_{III} = 0.13$ (α = 0.327, β = 0.533, γ = 0.14). As follows from Figure 1, the refinements introduced by the three-channel model have only a slight influence on the theoretical saturation curves because the first single-channel model has already given a good result, as suggested by Δ_I error value for both P and B curves.

Second sample (figure 2). Curve A_1: $R_{Sr} = 8 \cdot 10^{-7}$ m, $\Delta_I = 0.0291$. Curve P_1: $R_{Sr} = 4 \cdot 10^{-7}$ m, $\Delta_I = 0.320$. Curve P_2: $R_{Min} = 2 \cdot 10^{-7}$ m, $R_{Max} = 10 \cdot 10^{-7}$ m, $\Delta_{III} = 0.218$ (α = 0.39, β = 0.48, γ = 0.13). Refinement by the three-channel model for curve A is not done, because error Δ_I has been already small. For the P_2 curve, is accuracy of the fitting curve is significantly improved, as follows from the figure 2B.

Third sample (figure 3). Curve P_1: $R_{Sr} = 4.2 \cdot 10^{-7}$ m, $\Delta_I = 0.364$. Curve P_2: $R_{Min} = 2 \cdot 10^{-7}$ m, $R_{Max} = 8 \cdot 10^{-7}$ m, $\Delta_{III} = 0.244$ (α = 0.363, β = 0.427, γ = 0.21). Curve B_1: $R_{Sr} = 11.6 \cdot 10^{-7}$ м, $\Delta_I = 0.164$. Curve B_2: $R_{Min} = 7 \cdot 10^{-7}$ m, $R_{Max} = 16 \cdot 10^{-7}$ m, $\Delta_{III} = 0.106$ (α = 0.277, β = 0.433, γ = 0.29). Here, as follows from figures 3A and 3B, error for P_1 curve obtained according to single-channel model is significant; three-channel model reduces the error, but it still remains noticeable. For B_1 curve error is more than two times smaller, so the refinement made by using three-channel model does not cause significant improvement in the curve.

Fourth sample (figure 4). Curve A_1: $R_{Sr} = 6.2 \cdot 10^{-7}$ m, $\Delta_I = 0.0261$. Curve P_1: $R_{Sr} = 4.2 \cdot 10^{-7}$ m, $\Delta_I = 0.269$. Curve P_2: $R_{Min} = 2 \cdot 10^{-7}$ m, $R_{Max} = 8 \cdot 10^{-7}$ m, $\Delta_{III} = 0.177$ (α = 0.328, β = 0.482, γ = 0.19).

Curve B_1: $R_{Sr} = 11.6 \cdot 10^{-7}$ m, $\Delta_I = 0.224$. Curve B_2 $R_{Min} = 7 \cdot 10^{-7}$ m, $R_{Max} = 15 \cdot 10^{-7}$ m, $\Delta_{III} = 0.135$ ($\alpha = 0.31$, $\beta = 0.38$, $\gamma = 0.31$). As follows from figures 4A and 4B, A_1 curve gives a good description for the first set of experimental points. For the other two curves P_1 and B_1, errors are significant, the use of a three-channel model reduces them a little, but the result is not satisfactory.

Fifth sample (figure 5). Curve A_1: $R_{Sr} = 11.5 \cdot 10^{-7}$ m, $\Delta_I = 0.0474$. Curve P_1: $R_{Sr} = 4.2 \cdot 10^{-7}$ m, $\Delta_I = 0.416$. Curve P_2: $R_{Min} = 2 \cdot 10^{-7}$ m, $R_{Max} = 11 \cdot 10^{-7}$ m, $\Delta_{III} = 0.284$ ($\alpha = 0.371$, $\beta = 0.509$, $\gamma = 0.12$). Curve B_1: $R_{Sr} = 11.2 \cdot 10^{-7}$ m, $\Delta_I = 0.279$. Curve B_2: $R_{Min} = 8 \cdot 10^{-7}$ m, $R_{Max} = 15 \cdot 10^{-7}$ m, $\Delta_{III} = 0.16$ ($\alpha = 0.36$, $\beta = 0.37$, $\gamma = 0.27$). The situation is almost the same as in the previous case. Curve A_1 gives a good approximation for the first set of points. But for the other two curves P_1 and B_1 errors are still noticeable, and three-channel model does not improve approximation significantly.

Sixth sample (figure 6). Curve A_1: $R_{Sr} = 6.2 \cdot 10^{-7}$ m, $\Delta_I = 0.027$. Curve P_1: $R_{Sr} = 4.4 \cdot 10^{-7}$ m, $\Delta_I = 0.243$. Curve P_2: $R_{Min} = 2 \cdot 10^{-7}$ m, $R_{Max} = 10 \cdot 10^{-7}$ m, $\Delta_{III} = 0.167$ ($\alpha = 0.327$, $\beta = 0.533$, $\gamma = 0.14$). for the curve B_1 $R_{Sr} = 9 \cdot 10^{-7}$ m, $\Delta_I = 0.241$, for the curve B_2 $R_{Min} = 5 \cdot 10^{-7}$ m, $R_{Max} = 14 \cdot 10^{-7}$ m, $\Delta_{III} = 0.146$ ($\alpha = 0.306$, $\beta = 0.374$, $\gamma = 0.32$). The situation is similar to the two previous two cases. Curve A_1 gives a good approximation for the first point set. But for the other two curves P_1 and B_1 errors are noticeable, but not so big as in the previous cases, and three-channel model helps to reduce error, although this improvement is not significant.

Seventh sample (figure 7). Curve A_1: $R_{Sr} = 5.25 \cdot 10^{-7}$ m, $\Delta_I = 0.0278$. Curve P_1: $R_{Sr} = 6.4 \cdot 10^{-7}$ m, $\Delta_I = 0.0389$. Curve B_1 $R_{Sr} = 8 \cdot 10^{-7}$ m, $\Delta_I = 0.15$. Curve B_2: $R_{Min} = 4 \cdot 10^{-7}$ m, $R_{Max} = 12 \cdot 10^{-7}$ m, $\Delta_{III} = 0.0944$ ($\alpha = 0.29$, $\beta = 0.42$, $\gamma = 0.29$). For this sample, even the first stage of processing gives a completely satisfactory result. For curve B_1 refinement leads to error decrease.

Eighth sample (figure 8). Curve A_1: $R_{Sr} = 2.3 \cdot 10^{-7}$ м, $\Delta_I = 0.108$. Curve P_1: $R_{Sr} = 3.2 \cdot 10^{-7}$ m, $\Delta_I = 0.128$. Curve B_1: $R_{Sr} = 2.4 \cdot 10^{-7}$ m, $\Delta_I = 0.205$. No refinements are made, because the errors are small and as follows from figures 8A and 8B, the curves provide satisfactorily approximation of the corresponding point sets.

4. Conclusions

Presented experimental and analytical data shows that in contrast to [7], a distinguishing feature of the obtained outcomes is the presence of rather small errors at the first stage of processing (when using single-channel model). At the same time, the refinements performed at the second stage of processing (by means of three-channel model of the pore system) cause only slight error decrease. The results suggest that the channel distributions along the radial direction of the investigated coal samples are narrow and have a pronounced peaks close to the obtained average values.

However, it should be noted that for experiments we used relatively small coal specimens with volumes of the same order of magnitude. Due to the fractal properties of porous and dispersed media [5, 14] and, in particular, of the coal, the above conclusion probably cannot be extended to large specimens. For example, the findings described in [15] shows that the samples of different size may have different patterns of water saturation.

References

[1] Lykov A V 1954 *Transport Phenomena in Capillary-Porous Bodies* (Moscow: Gosizdat Publ.) p 296
[2] Beylin M I 1969 *Theoretical Basis of Coal Dewatering Processes* (Moscow: Nedra Publ.) p 240
[3] Churaev N V 1990 *Physicochemistry of mass transfer processes in porous bodies* (Moscow: Khimiya Publ.) p 272
[4] Barabanov V L 2014 Empirical parameters of the model of countercurrent capillary impregnation of rocks *J. Geophysical Research* **15** (1) pp 27-52
[5] Barabanov V L and Lyubushin A A 2013 Experience in the study of fractal properties of

capillary impregnation of rocks. *Engineering Physics Journal* **86** (1) pp 3-13
[6] Yelisieiev V, Lutsenko V, Demchenko T and Ruban V 2019. Empirical determination of water saturation of porous materials in the process of long duration imbibition. *E3S Web Conf. Int. Conf.* **109** 00117 DOI: 10.1051/e3sconf/201910900117
[7] Yelisieiev V, Lutsenko V and Berkout V 2022 Mathematical model of porous solid impregnation based on multichannel representation of the pore system *IOP Conf. Ser. Earth Environ. Sci.* 970 012023 DOI: 10.1088/1755-1315/970/1/012023
[8] Gaevoy V V 2000 Technologies of chemical desulphurization of coals M*ineral processing* (Dnipro: National Mining University) **8** (49) pp 100-110
[9] Aerov M E, Todes O M and Narinsky D A 1979 *Apparatus with a stationary granular layer* (Leningrad: Khimiya Publ.) p 176
[10] Kheifets L I and Neimark A V 1982 *Multiphase processes in porous media* (Moscow: Khimiya Publ.) p 320
[11] Entov V M 1992 Micromechanics of flow through porous media *J. Fluid Dyn.* **27** pp 824-833 DOI: 10.1007/BF01051359
[12] Voloshin V P, Medvedev N N and Fenelopov V B 1999 Study of the pore structure in computer models of dense and loose layers of spherical particles *J. of Structural Chemistry* **40** (4) pp 681-692
[13] Gyulmaliev A M Golovin G S and Gladun T G 2003 *Theoretical Foundations of Coal Chemistry* (Moscow: Moscow State Mining University Publ.) p 556
[14] Roldugin V I 2003 Fractal structures in dispersed systems *Russian Chemical Reviews* **72** (10) pp 931 – 960
[15] Nadutyy V P, Yelisieiev V I, Lutsenko V I and Kostyrya S V 2017 Experimental determination of the dependence of the water sediment of the milled mount mass from the sizes of pieces *Bul. of the National Technical University "KhPI". Ser.: New solutions in modern technology* (Kharkiv: NTU "KhPI" Publ.) **23** (1245), p 36-40 DOI: 10.20998/2413-4295.2017.23.06